Zeitschrift für Kristallographie 172, 297–314 (1985)

Tricalcium silicate $Ca_3O[SiO_4]$: The monoclinic superstructure

Fumito Nishi and Yoshio Takéuchi

Mineralogical Institute, Faculty of Science, University of Tokyo, Hongo, Tokyo 113, Japan

and Iwao Maki

Nagoya Institute of Technology, Gokiso-cho, Showa-ku, Nagoya 466, Japan

Received: June 20, 1985

Tricalcium silicate / Superstructure / Phase transition

Abstract. Crystals, free from twinning, of the monoclinic phase of tricalcium silicate exhibiting superstructure reflections have been obtained. Crystal data are: $a = 33.083(8)$, $b = 7.027(2)$, $c = 18.499(4)$ Å, $\beta = 94.12(2)°$, $Z = 36 \times Ca_{2.89}Mg_{0.11}OSiO_4$, $V = 4289$ Å^3. The structure analysis was carried out using 3886 independent reflection intensities measured on a single-crystal diffractometer. The unit cell ($a = 12.242$, $b = 7.027$, $c = 9.250$ Å, $\beta = 116.04°$) of the monoclinic expression of the rhombohedral average structure, contains six Ca's and a triplet of silicate tetrahedra which are successively arranged on the pseudothreefold axis. The mode of orientational disorder of these tetrahedra is found to be different from that of the corresponding tetrahedra in the rhombohedral phase **R**. The average structure has been successfully deconvoluted to yield the superstructure containing six triplets of tetrahedra in its cell; the structure has been refined to $R = 9.9\%$ (13.6% for 2818 superstructure reflections, and 5.9% for average structure). With regard to the mode of orientational disorder, the tetrahedra of certain triplets of the superstructure determined are similar with those of **R**, while others share features with those of the triclinic phase **T** (Golovastikov et al., 1975). Thus the orientational disorder of the tetrahedra that characterizes the superstructure has features intermediate between those of **R** and **T**. The coordination number of the Ca atoms (mean Ca–O = 2.41 Å) is in the range $6.0 \sim 7.12$, giving an overall average 6.15 which is also intermediate between those of **R** and **T**.

Introduction

Among various polymorphic forms of tricalcium silicates (C_3S), reported by Bigaré, Guinier, Mazières, Regourd, Yannaquis, Eysel, Hahn and Woermann (1967), Maki and Chromý (1978) and summarized by Nishi and Takéuchi (1984b), the structures of the triclinic room-temperature form and the rhombohedral high-temperature form at 1473 K have been studied by Golovastikov, Matveeva and Belov (1975) and Nishi and Takéuchi (1984b), respectively. The structural study of the latter form in particular elucidated marked features of the orientational disorder of the constituent tetrahedra, suggesting that the occurrence of various intermediate forms will presumably be explainable in terms of a stepwise change in mode of the orientational order-disorder of the tetrahedra (Takéuchi, Nishi and Maki, 1984).

Of intermediate forms, the monoclinic forms that occur in the temperature range 1253 K $\sim$ 1323 K may be stabilized to room-temperature by doping foreign components such as MgO, Al_2O_3 or others (Bigaré et al., 1967). In addition to the two monoclinic forms found by Bigaré et al. (1967), Maki and Chromý (1978) observed, based on optical study, the existence of a new monoclinic form $\mathbf{M_3}$, the seventh modification of C_3S. The X-ray single-crystal diffraction of this form exhibits highly complicated superstructure reflections corresponding to those of the crystal whose average structure was previously proposed by Jeffery (1952). This form can be stabilized at ambient temperature by doping MgO in an appropriate concentration. The crystals having this superstructure are in general obtained in a twinned form, thus making the problem of solving the structure highly difficult.

One of the present authors (I.M.), however, was successful in synthesizing crystals free from twinning. We have therefore undertaken the structural study of the monoclinic form exhibiting superstructure reflections with the result as reported in the present paper. A brief account on the structure has appeared earlier (Takéuchi, Nishi and Maki, 1984).

Experimental

The crystals were prepared starting with a mixture of C_3S doped with MgO and using $CaCl_2$ as a flux component. It was melted at 1623 K for 5 h until the flux was almost evaporated. The product was washed with ethanol to remove the flux attached. After a number of X-ray examinations with the precession method, several single-crystals free from twinning were successfully obtained (Fig. 1). Electron microprobe analyses showed that the crystals had a chemical composition $Ca_{2.89}Mg_{0.11}SiO_5$. A crystal piece having roughly the shape of a trapezoid plate, $0.5 \times 0.3 \times 0.04$ mm, was selected and used for the present study.

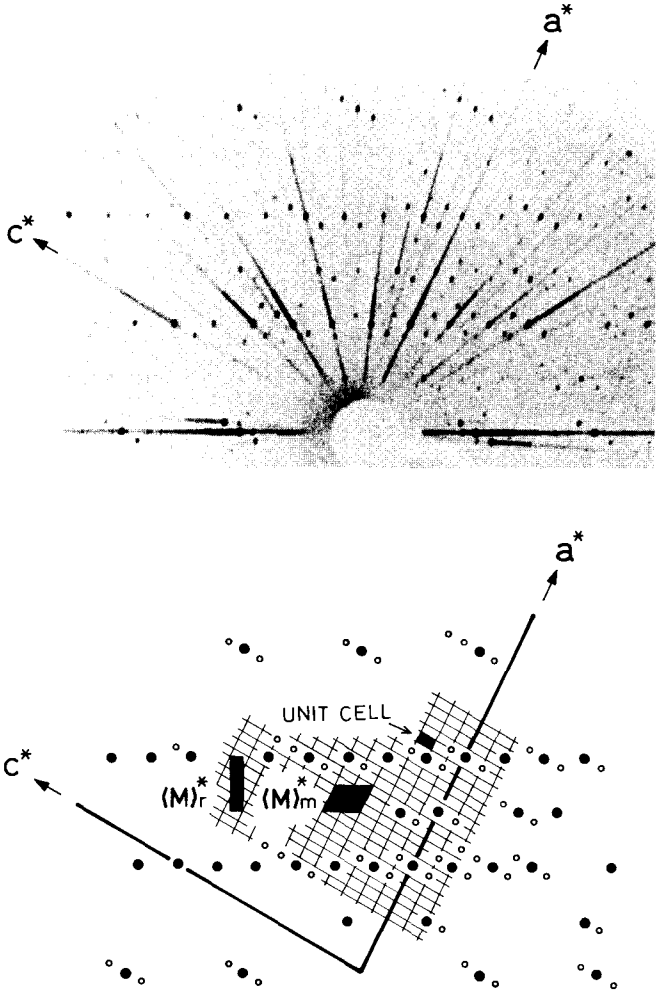

Fig. 1. Precession photograph showing *h0l* reflections (Mo*Kα*) (*top*) and portion of the corresponding reciprocal lattice (*bottom*). Average-structure reflections and satellites are indicated in the latter by solid and open circles, respectively. For reciprocal cells indicated by solid areas, see Fig. 2

The monoclinic cell dimensions were obtained by a least-squares procedure applied to the sin 2 θ values of 24 reflections measured with a Rigaku AFC-5 single crystal diffractometer, using graphaite monochromated Mo*Kα* radiation. They are a = 33.083(8) Å, b = 7.027(2) Å, c = 18.499(4) Å and β = 94.12(2)°. The unit cell contains 36 chemical units. As reported by Jeffery (1952) the structure has a rhombohedral sub-

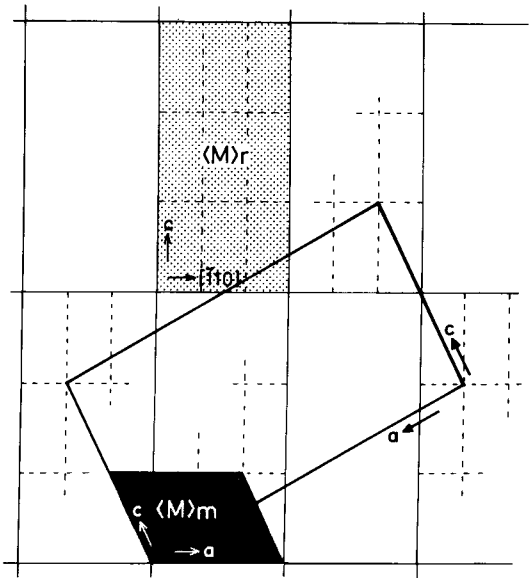

Fig. 2. The relationships between the monoclinic supercell (solid lines) and the cell of the rhombohedral average structure $<\mathbf{M}>_r$(stippled). The monoclinic representation of the latter $<\mathbf{M}>_m$ is indicated

structure (or average structure) $<\mathbf{M}>_r$ (Fig. 2), having calculated cell dimensions $a = 7.027$ Å and $c = 24.93$ Å and the space group $R3m$. As a consequence we may take a smaller monoclinic subcell with one of the axes corresponding to the translation along the long diagonal of the hexagonal cell of **R** (Fig. 2). We adopted this smaller monoclinic subcell, $a = 12.242$ Å, $b = 7.027$ Å, $c = 9.250$ Å and $\beta = 116.04°$, as working cell for subsequent structure analysis. This monoclinic substructure will be denoted $<\mathbf{M}>_m$ (Fig. 2).

The $\omega - 2\theta$ scan technique was used to measure, on the above-mentioned single-crystal diffractometer, half the number of the Mo$K\alpha$ diffraction intensities up to $2\theta = 60°$. A closer examination of each F(hkl) and F($h\bar{k}l$) pair among a total of 12500 diffraction intensities thus collected confirmed the monoclinic symmetry of the crystal. The possible space groups are Cm or $C2/m$. The structure factors were cut-off at the $3\sigma(|F_o|)$ level, and those having intensities whose backgrounds were unusually asymmetrical were omitted. Then by averaging each pair, F(hkl) and F($h\bar{k}l$), we obtained a total of 3886 independent structure factors; the range of h, k, l was $-46 \leqq h \leqq 45$, $0 \leqq k \leqq 9$, $-26 \leqq l \leqq 0$. Among them the number of superstructure reflections was 2818. The deviations of $|F_o|$ of three reference reflections were within 2.2% throughout the intensity collection.

Determination of the average structure

Preliminary analysis

The structure analysis was initiated with the determination of the monoclinic average structure based on a total of 1068 structure factors of low order average-structure reflections.

The initial atomic parameters for the monoclinic average structue were obtained by folding the rhombohedral structure at 1473 K (Nishi and Takéuchi, 1984b) into its monoclinic subcell. There are two possible space groups for the monoclinic structure; one being noncentric *Cm* and the other centric *C*2/*m*. By means of isotropic refinements with the use of the least-squares program ORFLS (Busing, Martin and Levy, 1962), the structure was refined to $R = 14.0\%$ and $R = 16.6\%$ in the space groups *Cm* and *C*2/*m*, respectively. In both cases, however, some of the Si–O bond lengths showed anomalous lengths such as 1.41 Å or 1.81 Å and some temperature factors very high values such as 10 $Å^2$. We adopted *Cm* for subsequent structural analysis partly because of the relatively low *R* value and partly *Cm* is a subgroup of *R*3*m* for the rhombohedral phase.

Determination of orientational disorder of tetrahedra

In the structures of C_3S as well as C_3G, the tetrahedra have a trend of orientational disorder as found in the rhombohedral structure of C_3S (Nishi and Takéuchi, 1984b) and the two-layer structure of C_3G (Nishi and Takéuchi, 1984a); a fraction of the tetrahedron pointing up the *c* direction (a U orientation), while the remaining fraction down *c* (a D orientation). Accordingly we have to determine such an orientational disorder of tetrahedra in the present monoclinic average structure.

The unit cell of the monoclinic average structure contains three silicate tetrahedra. They successively occur on a pseudothreefold axis [Fig. 3(a)]. Such a linear arrangement of the triplet of tetrahedra can be regarded as one of the basic features of the structures of the polymorphic forms of C_3S in general. This means that the arrangement of tetrahedra in the structure of a given polymorph can be described in terms of the triplet.

Now, consider a given triplet consisting of three tetrahedra having the same orientation (e.g. U orientation) with respect to the pseudothreefold axis [Fig. 3(a)]. Then suppose that the sense of orientation of the top tetrahedron is inverted, namely takes a D orientation. The remaining two tetrahedra should also necessarily invert their sense of orientation because of steric restrictions existing among the linear arrangement. This situation means that the orientation of the central tetrahedron, Si(1), is controlled by those of the top tetrahedron, Si(2), and the bottom Si(3). Accordingly, in the preliminary cycles of anisotropic refinement applying the occupancy (or orientational) parameters of the U–D pairs of each tetrahedron, those

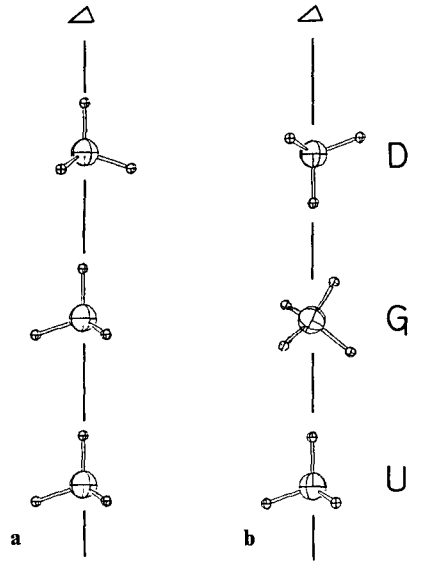

Fig. 3. Two basic modes of relative orientations of a triplet of tetrahedra on the pseudo-threefold axis (open triangle). (**a**) An example of the same orientation (a case of U orientation is shown). (**b**) A case in which the central tetrahedron takes the G orientation

parameters of Si(2) and Si(3) were varied, while the orientation of Si(1) was fixed as obtained by the above isotropic refinement. For calculations, the configuration of each tetrahedron was constrained to the shape of a regular tetrahedron with Si−O = 1.63 Å and O−Si−O angle = 109.5°.

The result revealed that the top tetrahedron showed about 70% D orientation and the bottom about 80% U. It follows that the permissible occupancies of the U or D orientations for the central tetrahedron are about 50%; the remaining fraction of about 50% must take some orientation other than U or D [in general, if the top tetrahedron shows p% D orientation and the bottom q% U, the permissible U or D orientation of the central tetrahedron is given by $(100-p)$% or $(100-q)$%, respectively]. As a model for such an orientation we adopted the one which has been found in the triclinic phase (Golovastikov et al., 1975). As will be observed in Fig. 3(b), the central tetrahedra of some of the triplets in the triclinic structure have such an orientation that is neither U nor D. We denoted this specific orientation by the symbol G [Fig. 3(b)].

Assuming, as an initial model, such a G orientation by 50% for our central tetrahedron, we then refined orientational parameters of all the tetrahedra with the use of ORFLS (Busing et al., 1962). The calculation finally converged to give an R = 8.4% for all reflections used. The resulting

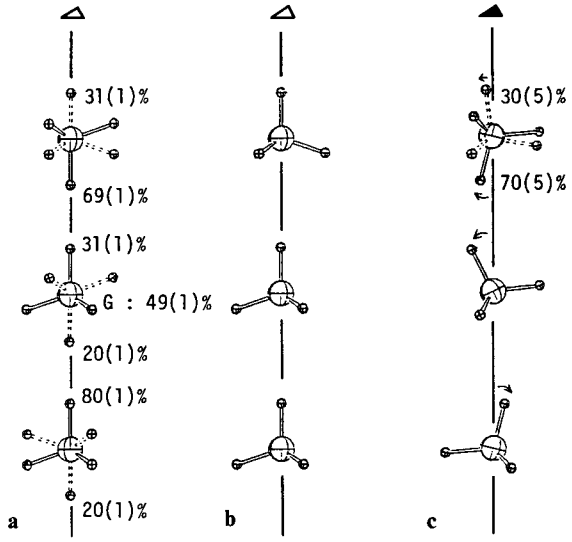

Fig. 4. The relative orientations of the triplet of tetrahedra of the monoclinic average structure: (**a**) present result, (**b**) Jeffery model (Jeffery, 1952). They are compared with those of the rhombohedral phase (Nishi and Takéuchi, 1984) (**c**). For each tetrahedron taking a statistical orientation, the occupancies of the fractions of the tetrahedron are indicated. The fraction of the central tetrahedron that takes the G orientation is not illustrated in (*a*)

triplet of the average structure is compared in Fig. 4 with the one proposed by Jeffery (1952) and that of the rhombohedral structure. When we note the mode of the arrangement of only Ca and Si, it is basically the same as the rhombohedral structure (Nishi and Takéuchi, 1984b) and the Jeffery model for the average structure of the true superstructure (Jeffery, 1952). So far as the orientational behavior of the tetrahedra is concerned, however, the Jeffery model is not acceptable.

Deconvolution of the average structure

The above structural features suggest that the true superstructure is basically defined by a specific mode of orientational order and disorder of the tetrahedra. The problem is now reduced to deconvolute the average triplet of tetrahedra to determine the orientational modes of eighteen tetrahedra in the sixfold multiple cell (if referred to the rhombohedral subcell, the true cell is fourfold). The deconvolution was made based on the following considerations:

(1) The fact that the bottom tetrahedron of the triplet of the average structure has 80% U orientation suggests that one of the six tetrahedra at

Table 1a. Fractional atomic coordinates ($\times 10^4$) and equivalent isotropic temperature factors

Atom	x	y	z	B_{eq}(Å^2)	Atom	x	y	z	B_{eq}(Å^2)
Ca(1A)	0075(8)	0	0090(12)	4.0	Ca(24A)	2435(3)	2491(14)	7443(4)	0.5
Ca(1B)	0024(8)	0	0056(12)		Ca(24B)	2468(3)	2347(13)	7554(4)	
Ca(2A)	6672(3)	0	1751(6)	0.1	Ca(25A)	0052(2)	2343(11)	−1589(4)	0.1
Ca(2B)	6673(3)	0	1741(6)		Ca(25B)	0051(2)	2338(11)	−1501(4)	
Ca(3A)	3240(4)	0	3330(7)	1.0	Ca(26A)	6704(2)	2318(11)	0073(4)	0.2
Ca(3B)	3193(4)	0	3307(7)		Ca(26B)	6771(2)	2306(11)	0144(4)	
Ca(4A)	0020(3)	0	5044(6)	0.4	Ca(27A)	3354(2)	2257(11)	1731(4)	0.3
Ca(4B)	−0133(4)	0	4971(6)		Ca(27B)	3365(2)	2385(12)	1853(4)	
Ca(5A)	6640(5)	0	6714(8)	0.6	Ca(28A)	−0047(2)	2281(11)	3417(4)	0.2
Ca(5B)	6632(4)	0	6697(8)		Ca(28B)	0018(2)	2540(12)	3490(4)	
Ca(6A)	3428(5)	0	8352(7)	1.6	Ca(29A)	6630(3)	2288(14)	5097(5)	0.9
Ca(6B)	3301(5)	0	8213(7)		Ca(29B)	6688(3)	2292(14)	5147(5)	
Ca(7A)	5973(3)	0	−0611(6)	0.2	Ca(30A)	3350(3)	2592(12)	6750(5)	0.7
Ca(7B)	5911(3)	0	−0691(6)		Ca(30B)	3360(3)	2165(12)	6827(5)	
Ca(8A)	2611(6)	0	0952(10)	2.5	Ca(31A)	8294(3)	2577(15)	−0192(5)	1.2
Ca(8B)	2568(5)	0	0864(9)		Ca(31B)	8306(3)	2893(14)	−0026(5)	
Ca(9A)	−0801(4)	0	2667(8)	1.3	Ca(32A)	4840(3)	2722(15)	1583(7)	1.8
Ca(9B)	−0810(4)	0	2644(8)		Ca(32B)	4905(3)	2303(15)	1584(7)	
Ca(10A)	5874(4)	0	4390(7)	0.9	Ca(33A)	1468(3)	2503(16)	3304(5)	1.4
Ca(10B)	5856(4)	0	4369(7)		Ca(33B)	1562(3)	2900(14)	3320(5)	
Ca(11A)	2575(4)	0	5989(6)	0.2	Ca(34A)	8167(3)	2762(12)	4875(4)	0.6
Ca(11B)	2561(3)	0	5976(6)		Ca(34B)	8224(3)	2520(14)	4918(5)	

Table 1a. (Continued)

Atom	x	y	z	B_{eq}(Å^2)	Atom	x	y	z	B_{eq}(Å^2)
Ca(12A)	−0742(4)	0	7698(7)	0.6	Ca(35A)	4941(3)	2858(13)	6505(4)	0.9
Ca(12B)	−0743(4)	0	7689(7)		Ca(35B)	4893(3)	2759(14)	6649(4)	
Ca(13A)	7356(3)	0	−1037(6)	0.3	Ca(36A)	1569(2)	2749(10)	8198(4)	0.1
Ca(13B)	7413(3)	0	−0957(6)		Ca(36B)	1643(2)	2675(10)	8283(4)	
Ca(14A)	4000(7)	0	0792(13)	3.9	Si(1)	0833(4)	0	4288(7)	2.1
Ca(14B)	3982(7)	0	0706(13)		Si(2)	2384(2)	0	−0838(4)	0.3
Ca(15A)	0651(4)	0	2486(7)	0.9	Si(3)	4292(3)	0	7460(6)	1.5
Ca(15B)	0628(4)	0	2445(7)						
Ca(16A)	7286(5)	0	4010(10)	1.8	Si(4)	5699(2)	0	7506(4)	0.2
Ca(16B)	7272(5)	0	4042(9)		Si(5)	−0943(2)	0	0741(4)	0.1
Ca(17A)	4004(4)	0	5711(9)	1.4	Si(6)	−1015(3)	0	5918(6)	1.5
Ca(17B)	3984(4)	0	5675(9)		Si(7)	0966(2)	0	−0851(4)	0.5
Ca(18A)	0694(4)	0	7491(9)	1.5	Si(8)	1637(3)	0	1591(5)	1.0
Ca(18B)	0647(4)	0	7349(9)		Si(9)	1628(2)	0	6629(4)	0.3
Ca(19A)	−0846(3)	2988(14)	−0926(5)	1.0	Si(10)	2340(4)	0	4118(8)	3.8
Ca(19B)	−0793(3)	2677(14)	−0789(5)		Si(11)	4214(3)	0	2509(5)	1.5
Ca(20A)	5799(4)	3018(15)	0884(6)	1.6	Si(12)	5008(3)	0	0039(5)	0.7
Ca(20B)	5850(3)	2058(15)	1013(5)		Si(13)	4975(4)	0	5004(7)	2.5
Ca(21A)	2411(2)	2447(12)	2470(4)	0.2	Si(14)	5682(2)	0	2442(4)	0.3
Ca(21B)	2459(3)	2559(13)	2501(4)		Si(15)	7600(2)	0	0882(4)	0.2
Ca(22A)	−0941(2)	2566(11)	4130(4)	0.2	Si(16)	7563(2)	0	5803(4)	0.2
Ca(22B)	−0885(2)	2550(12)	4273(4)		Si(17)	−1748(3)	0	3338(4)	0.4
Ca(23A)	5744(2)	2726(13)	5851(5)	0.8	Si(18)	−1693(2)	0	−1575(4)	0.2
Ca(23B)	5784(3)	2399(14)	5943(5)						

Table 1b. The fractional coordinates of the oxygen atoms ($\times 10^3$) and isotropic temperature factors (those from D11 down to U66 are equivalent temperature factors)

Site	Occupancy	x	y	z	B(Å^2)	Site	Occupancy	x	y	z	B(Å^2)
1A	0.5	990(3)	0	245(5)	4.2(8)	U95	0.32	212	0	681	1.3(3)
1B	0.5	988(3)	0	245(5)	4.2(8)	U96	0.32	141	189	627	1.3(3)
2A	0.5	038(3)	0	119(4)	3.8(11)	G91	0.045	140	050	584	1.3(3)
2B	0.5	052(3)	0	124(5)	3.8(11)	G92	0.045	133	−123	712	1.3(3)
3A	0.5	030(2)	0	599(3)	2.8(9)	G93	0.045	204	−123	655	1.3(3)
3B	0.5	038(2)	0	610(4)	2.8(9)	G94	0.045	175	197	706	1.3(3)
4A	0.5	−004(2)	0	753(3)	1.0(3)	D101	0.59	255	0	335	11(4)
4B	0.5	−005(2)	0	754(3)	1.0(3)	D102	0.59	268	0	480	2.7(8)
5A	0.5	372(2)	0	−077(3)	2.8(9)	D103	0.59	206	189	415	2.0(5)
5B	0.5	373(2)	0	−047(4)	2.8(9)	U104	0.41	212	0	487	6(3)
6A	0.5	329(3)	0	075(4)	4.1(8)	U105	0.41	283	0	430	2(1)
6B	0.5	331(3)	0	077(5)	4.1(8)	U106	0.41	221	189	365	3(1)
7A	0.5	289(2)	0	211(4)	2.7(7)	D111	0.57	444	0	175	5(2)
7B	0.5	289(2)	0	223(4)	2.7(7)	D112	0.57	372	0	233	3(1)
8A	0.5	362(1)	0	441(2)	0.8(3)	D113	0.57	435	189	298	3(1)
8B	0.5	362(1)	0	442(2)	0.8(3)	U114	0.43	399	0	327	5(2)
9A	0.5	325(1)	0	583(2)	0.1(4)	U115	0.43	382	0	193	5(2)
9B	0.5	334(1)	0	595(2)	0.1(4)	U116	0.43	450	189	257	2.3(8)
10A	0.5	282(1)	0	724(3)	1.4(5)	U124	0.43	478	0	080	6(1)
10B	0.5	293(2)	0	732(3)	1.4(5)	U125	0.43	550	0	022	6(1)
11A	0.5	666(1)	0	−093(2)	0.5(4)	U126	0.43	487	189	−043	6(1)
11B	0.5	675(1)	0	−081(2)	0.5(4)	G121	0.285	478	050	−075	6(1)
12A	0.5	627(2)	0	049(3)	1.5(6)	G122	0.285	466	−123	040	6(1)
12B	0.5	634(2)	0	067(3)	1.5(6)	G123	0.285	542	−123	−004	6(1)
13A	0.5	706(2)	0	285(4)	2.6(6)	G124	0.285	513	197	047	6(1)
13B	0.5	704(2)	0	290(4)	2.6(6)	D131	0.37	520	0	425	3.4(6)
14A	0.5	648(2)	0	421(3)	2.1(7)	D132	0.37	448	0	483	3.4(6)
14B	0.5	655(2)	0	414(3)	2.1(7)	D133	0.37	511	189	547	3.4(6)
15A	0.5	608(1)	0	564(3)	1.5(6)	G131	0.315	520	050	580	3.4(6)
15B	0.5	622(2)	0	567(3)	1.5(6)	G132	0.315	526	−128	451	3.4(6)
16A	0.5	705(1)	0	763(3)	1.4(5)	G133	0.315	456	−123	508	3.4(6)
16B	0.5	709(2)	0	771(3)	1.4(5)	G134	0.315	481	197	463	3.4(6)
[redacted]											
17A	0.5	949(2)	0	376(3)	1.5(6)	D141	0.37	591	0	169	16(9)
17B	0.5	957(2)	0	401(3)	1.5(6)	D142	0.37	602	0	212	12(7)
		-0-								-0-	
		057(2)								312	

Site	Occupancy	x	y	z	B(Å^2)	Site	Occupancy	x	y	z	B(Å^2)
18A	0.5	960(1)	0	897(2)	0.8(4)	D143	0.37	540	189	248	2.4(7)
18B	0.5	965(1)	0	907(2)	0.8(4)	U144	0.63	546	0	320	12(5)
D11	1.0	111(2)	0	357(3)	8.1	U145	0.63	617	0	262	6(2)
D12	1.0	035(2)	0	408(3)	4.2	U146	0.63	555	189	197	16(4)
D13	1.0	096(1)	187(5)	474(2)	3.2	D151	0.22	782	0	013	11(7)
U24	1.0	215(1)	0	−011(2)	0.5	D152	0.22	711	0	070	4(3)
U25	1.0	286(1)	0	−063(2)	2.9	D153	0.22	773	189	135	2(1)
U26	1.0	226(1)	184(4)	−133(1)	2.1	U154	0.78	738	0	164	6(1)
D31	1.0	450(1)	0	668(2)	1.7	U155	0.78	726	0	020	2.4(6)
D32	1.0	379(1)	0	730(2)	2.3	U156	0.78	788	189	085	3.2(6)
D33	1.0	443(1)	183(3)	791(1)	1.6	D161	0.93	778(1)	0	505(1)	0.4(3)
U44	1.0	549(1)	0	830(2)	2.1	D162	0.93	707(1)	0	565(1)	0.5(3)
U45	1.0	616(1)	0	767(2)	1.5	D163	0.93	769(1)	191(3)	626(1)	1.4(3)
U46	1.0	555(1)	188(3)	704(1)	2.0	U164	0.07	734	0	656	0.8(2)
U54	1.0	−118(1)	0	149(2)	1.5	U165	0.07	717	0	522	0.8(2)
U55	1.0	−044(1)	0	093(2)	1.2	U166	0.07	787	180	594	0.8(2)
U56	1.0	−107(1)	187(3)	027(1)	2.7	U174	0.07	−197	0	409	4.6(9)
U64	1.0	−123(1)	0	669(2)	4.7	U175	0.07	−126	0	352	4.6(9)
U65	1.0	−054(1)	0	608(2)	3.8	U176	0.07	−188	189	287	4.6(9)
U66	1.0	−117(1)	186(4)	542(2)	2.3	G171	0.2325	−197	050	255	4.6(9)
D71	0.68	119	0	−161	0.7(4)	G172	0.2325	−204	−123	383	4.6(9)
D72	0.68	048	0	−103	1.6(6)	G173	0.2325	−134	−123	326	4.6(9)
D73	0.68	110	189	−038	3.9(7)	G174	0.2325	−163	197	377	4.6(9)
U74	0.32	074	0	−009	4(2)	G175	0.2325	−152	050	413	4.6(9)
U75	0.32	055	0	−138	2(1)	G176	0.2325	−145	−123	285	4.6(9)
U76	0.32	125	189	−073	1.9(8)	G177	0.2325	−216	−123	342	4.6(9)
G81	0.5	141	050	080	3.5(4)	G178	0.2325	−187	197	291	4.6(9)
G82	0.5	134	−123	208	3.5(4)	U184	0.78	−192	0	−082	2.0(3)
G83	0.5	205	−123	151	3.5(4)	U185	0.78	−120	0	−140	2.0(3)
G84	0.5	176	197	202	3.5(4)	U186	0.78	−183	189	−204	2.0(3)
D91	0.59	185	0	587	1.3(3)	G181	0.11	−192	050	−237	2.0(3)
D92	0.59	114	0	645	1.3(3)	G182	0.11	−199	−123	−108	2.0(3)
D93	0.59	176	189	710	1.3(3)	G183	0.11	−128	−123	−165	2.0(3)
U94	0.32	140	0	739	1.3(3)	G184	0.11	−158	210	−125	2.0(3)

the corresponding positions of the six subcells would have a D orientation, the remaining U orientation.

(2) The U to D ratio of the top tetrahedron of the average structure nearly corresponds to the case in which two, among six tetrahedra of this category in the cell, are in the U orientation and four in D.

(3) Once the orientations of the top and bottom tetrahedra in the triplet of a subcell are assumed, the possible orientation of the central tetrahedron can be fixed as mentioned previously.

These considerations gave 15 possible sets of average structures of the six triplets in the supercell. In addition, we assumed the case in which the U to D ratio of the top tetrahedron of the average triplet was not 2:4 but 1:5, giving six additional models for the superstructure.

Structure factors corresponding to 10 strongest superstructure reflections were then calculated for a total of the 21 models thus derived. One model which graphically showed a best fit between F_o and F_c was chosen as the starting model for structure determination. A number of repetitions of Fourier and difference Fourier syntheses and least-squares calculations successfully gave an R as low as 9.9% for 3886 reflections used; R = 13.6% for 2818 superstructure reflections and 5.9% for 1068 average-structure reflections. At initial stage of calculations, the shape of all tetrahedra was constrained to a regular tetrahedron, as mentioned before. Later, however, seven tetrahedra out of 18 were found to have perfectly or almost perfectly ordered orientations; the constraint to these tetrahedra were therefore released at the final stage of refinement. The final atomic parameters are listed in Table 1. In this table, a pair of the split positions for each Ca (and separate oxygen atom) are denoted A and B. The symbols for the oxygen atoms are given as in the case of the rhombohedral structure (Nishi and Takéuchi, 1984b).

Description and discussion

General features of the structure

The monoclinic superstructure of C_3S thus obtained is illustrated in Fig. 5(a) and Fig. 5(b). In the structure the Si atoms and part of the Ca atoms are located on the mirror planes at x, 0, z and x, $\frac{1}{2}$, z, the remaining Ca atoms being located very closely in a plane between the above two mirror planes. We may thus regard the structure to consist of two alternate layers, parallel to (010), with distance of 1.75 Å, one consisting of the silicate tetrahedra and Ca's, and the other only of Ca's.

If we exclude oxygen atoms which are associated to Si atoms and note the distribution of Si, Ca and separate oxygen atoms, we readily observe the existence of pseudo centers of symmetry at the locations which may be classified into three categories; (1) those on the central Si of each triplet,

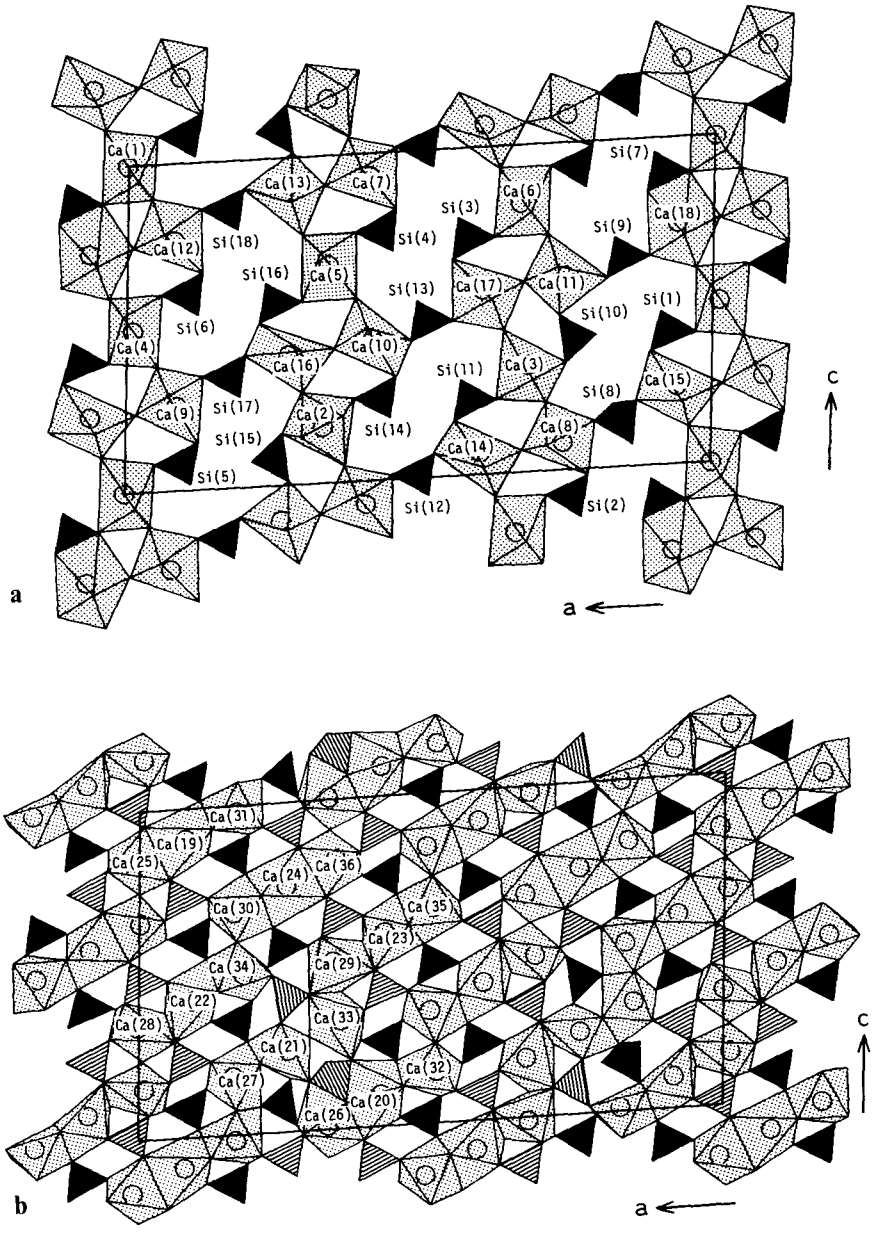

Fig. 5. The monoclinic superstructure, viewed down *b*. (**a**) The arrangement of the polyhedra about Ca and Si in the mirror plane at the $y = 0$ level. (**b**) The arrangement of the polyhedra about Ca at the $y \simeq \frac{1}{4}$ level [the Si tetrahedra at $y = 0$ (solid triangle) and those at $y = \frac{1}{2}$ (ruled) are shown together]. Each tetrahedron is represented by the one which has the orientation of the highest fraction. The splittings of Ca are not indicated

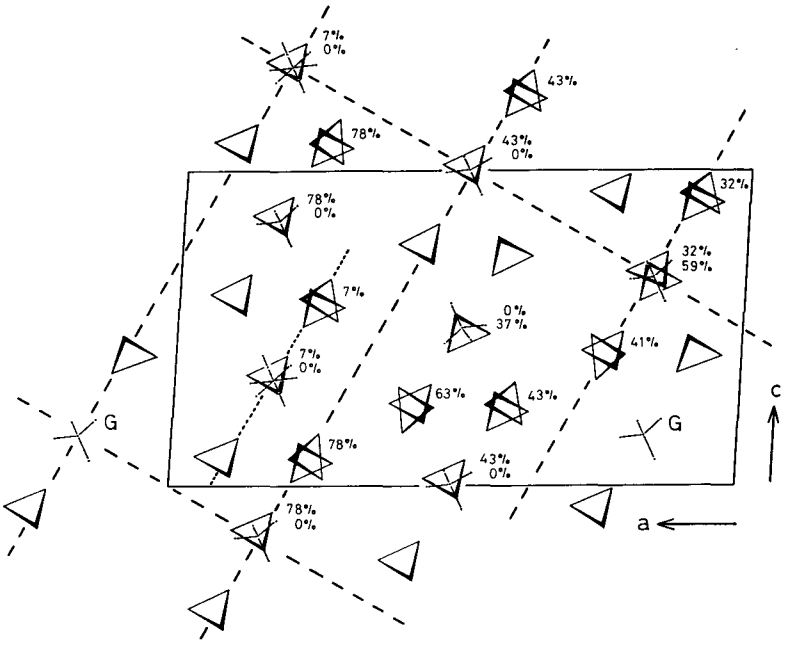

Fig. 6. Details of the orientational disorder of the silicate tetrahedra at $y = 0$. The broken lines trace the cells of the rhombohedral average structure; the location of one of the pseudo-threefold axes is indicated by a dotted line. For tetrahedra which show U–D disorder, the fractions of U are indicated. While for those which show U – D – G disorder, fractions of U and D are indicated, the first line in each set of two figures showing the U fraction. The tetrahedra to which no figures are associated have ordered orientation. The origin of the corresponding figure in Takéuchi et al. (1984) is taken on a Si atom

(2) those on the central oxygen atom of each linear set of three separate oxygen atoms, and (3) those on certain Ca atoms as shown in Fig. 5(a) and Fig. 5(b). (In the triclinic structure some of them become true symmetry).

The structures of the rhombohedral phase and the triclinic phase share features in common. Presumably these features are common in all polymorphic forms in C_3S. Note that the above-mentioned layers are different from the unit layer on which the theory of polytypism of C_3G is based (Nishi and Takéuchi, 1985); when referred to the monoclinic supercell the unit layer is parallel to $(\bar{1}01)$.

Orientational order and disorder of the tetrahedra

Now, the salient feature that characterizes the superstructure is in the mode of orientational order and disorder of the constituent silicate tetrahedra. As observed in Fig. 6, among eighteen tetrahedra in the unit cell six have

Table 2. Si–O bond lengths, O–Si–O angles and O–O distances of the tetrahedra showing ordered or nearly ordered U or D orientations (see Table 3)

Si	Oxygen	Bond length	O–Si–O angle			O–O distance
Si(1)	D11	1.67(6) Å	D11	Si1 D12	114(3)°	2.75(9) Å
	D12	1.60(6)	D11	D13	106(2)×2	2.62(6)×2
	D13	1.60(4)×2	D12	D13	110(2)×2	2.62(6)×2
	Mean	1.62	D13	D13	111(2)	2.62(5)
Si(2)	U24	1.61(3) Å	U24	Si2 U25	109(2)°	2.61(5) Å
	U25	1.59(3)	U24	U26	111(1)×2	2.66(3)×2
	U26	1.62(2)×2	U25	U26	110(1)×2	2.64(3)×2
	Mean	1.61	U26	U26	106(1)	2.59(3)
Si(3)	D31	1.65(3) Å	D31	Si3 D32	109(2)°	2.69(5) Å
	D32	1.65(3)	D31	D33	110(1)×2	2.64(3)×2
	D33	1.58(2)×2	D32	D33	110(1)×2	2.64(3)×2
	Mean	1.62	D33	D33	109(1)	2.58(3)
Si(4)	U44	1.67(3) Å	U44	Si4 U45	108(2)°	2.59(5) Å
	U45	1.54(3)	U44	U46	110(1)×2	2.69(3)×2
	U46	1.63(2)×2	U45	U46	111(1)×2	2.60(3)×2
	Mean	1.62	U46	U46	109(1)	2.64(3)
Si(5)	U54	1.63(4) Å	U54	Si5 U55	110(2)°	2.71(5) Å
	U55	1.67(3)	U54	U56	109(1)×2	2.64(4)×2
	U56	1.61(2)×2	U55	U56	110(1)×2	2.69(3)×2
	Mean	1.63	U56	U56	109(1)	2.63(3)
Si(6)	U64	1.64(4) Å	U64	Si6 U65	109(2)°	2.62(5) Å
	U65	1.58(3)	U64	U66	110(1)×2	2.70(5)×2
	U66	1.66(3)×2	U65	U66	112(1)×2	2.68(5)×2
	Mean	1.64	U66	U66	104(2)	2.62(4)
Si(16)	D161	1.61(2) Å	D161	Si16 D162	111(1)°	2.68(2) Å
	D162	1.64(2)	D161	D163	110(1)×2	2.65(2)×2
	D163	1.63(2)×2	D162	D163	108(1)×2	2.64(2)×2
	Mean	1.63	D163	D163	111(1)	2.69(2)

fixed orientation of either U or D with respect to the *c* axis of the rhombohedral subcell (the direction corresponds to [$\bar{2}$07] referred to the true monoclinic cell). The remaining twelve tetrahedra show statistical orientations, each being defined in terms of U, D and G orientations.

The mode of arrangement of these individual tetrahedra may be simplified by looking at them as that of six triplets of tetrahedra as mentioned previously. They are arranged parallel to the *c* axis of the rhombohedral subcell. A closer examination into the triplets reveals that some of them, e.g. Si(3)–Si(13)–Si(14), are closely similar to the one we found in the rhombohedral phase **R** (Nishi and Takéuchi, 1984b), while some others, e.g. Si(1)–Si(8)–Si(2), are similar to those in the triclinic phase **T** (Golovastikov et al., 1975). Accordingly we can say that the

Table 3. Ratios of the orientational disorder of tetrahedra

Tetrahedron	D orientation (%)	U orientation (%)	G orientation (%)
Si(1)	100		
Si(2)		100	
Si(3)	100		
Si(4)		100	
Si(5)		100	
Si(6)		100	
Si(7)	68(2)	32(2)	
Si(8)			100
Si(9)	59(3)	32(2)	9(3)
Si(10)	59(3)	41(3)	
Si(11)	57(3)	43(3)	
Si(12)		43(3)	57(3)
Si(13)	37(3)		63(3)
Si(14)	37(3)	63(3)	
Si(15)	22(2)	78(2)	
Si(16)	93(2)	7(2)	
Si(17)		7(2)	93(2)
Si(18)		78(2)	22(2)

Table 4. Splitting distances of Ca and separate oxygen atoms (Å)

Ca(1A) – Ca(1B)		0.18(4)	Ca(19)A – Ca(19B)		0.37(1)	O(1A) – O(1B)		0.1(1)
2A –	2B	0.02(1)	20A –	20B	0.73(2)	2A –	2B	0.5(1)
3A –	3B	0.16(2)	21A –	21B	0.18(1)	3A –	3B	0.3(1)
4A –	4B	0.52(2)	22A –	22B	0.31(1)	4A –	4B	0.1(1)
5A –	5B	0.04(2)	23A –	23B	0.31(1)	5A –	5B	0.55(9)
6A –	6B	0.48(2)	24A –	24B	0.25(1)	6A –	6B	0.1(1)
7A –	7B	0.24(1)	25A –	25B	0.16(1)	7A –	7B	0.2(1)
8A –	8B	0.21(3)	26A –	26B	0.25(1)	8A –	8B	0.1(1)
9A –	9B	0.05(2)	27A –	27B	0.24(1)	9A –	9B	0.36(5)
10A –	10B	0.07(2)	28A –	28B	0.31(1)	10A –	10B	0.39(8)
11A –	11B	0.05(2)	29A –	29B	0.21(1)	11A –	11B	0.37(5)
12A –	12B	0.02(2)	30A –	30B	0.33(1)	12A –	12B	0.38(9)
13A –	13B	0.23(1)	31A –	31B	0.38(1)	13A –	13B	0.1(1)
14A –	14B	0.17(4)	32A –	32B	0.37(2)	14A –	14B	0.26(9)
15A –	15B	0.10(2)	33A –	33B	0.42(1)	15A –	15B	0.46(8)
16A –	16B	0.08(3)	34A –	34B	0.26(1)	16A –	16B	0.20(8)
17A –	17B	0.09(2)	35A –	35B	0.33(1)	17A –	17B	0.53(9)
18A –	18B	0.30(2)	36A –	36B	0.29(1)	18A –	18B	0.23(5)

present superstructure has features intermediate between the structures of the high-temperature **R** and room-temperature **T**.

The bond lengths and bond angles we obtained for the ordered tetrahedra are listed in Table 2 and the ratios of the orientational disorder of each tetrahedron in Table 3.

Table 5. Ca – O bond lengths (Å)

	Coord. number	Range	Mean		Coord. number	Range	Mean
Ca(1)	6.00	2.26 – 2.93	2.44	Ca(19)	6.29	2.21 – 2.79	2.45
Ca(2)	7.00	2.20 – 2.97	2.53	Ca(20)	6.50	2.21 – 2.88	2.47
Ca(3)	6.00	2.20 – 2.96	2.45	Ca(21)	6.00	2.28 – 2.88	2.38
Ca(4)	6.63	2.25 – 2.99	2.49	Ca(22)	6.00	2.34 – 2.95	2.46
Ca(5)	6.09	2.21 – 2.99	2.40	Ca(23)	6.05	2.24 – 2.97	2.33
Ca(6)	7.12	2.22 – 2.90	2.44	Ca(24)	6.00	2.25 – 3.00	2.39
Ca(7)	6.00	2.25 – 2.59	2.40	Ca(25)	6.00	2.25 – 2.84	2.38
Ca(8)	6.00	2.29 – 2.47	2.38	Ca(26)	6.50	2.23 – 2.91	2.44
Ca(9)	6.00	2.26 – 2.46	2.38	Ca(27)	6.40	2.22 – 3.00	2.42
Ca(10)	6.00	2.20 – 2.48	2.33	Ca(28)	6.00	2.26 – 2.52	2.39
Ca(11)	6.00	2.21 – 2.54	2.36	Ca(29)	6.00	2.24 – 2.78	2.42
Ca(12)	6.00	2.32 – 2.66	2.40	Ca(30)	6.00	2.24 – 2.87	2.39
Ca(13)	6.00	2.26 – 2.61	2.36	Ca(31)	6.00	2.21 – 2.54	2.33
Ca(14)	6.00	2.28 – 2.62	2.41	Ca(32)	6.00	2.30 – 2.70	2.40
Ca(15)	6.00	2.32 – 2.62	2.44	Ca(33)	6.00	2.28 – 2.63	2.42
Ca(16)	6.00	2.21 – 2.56	2.37	Ca(34)	6.00	2.26 – 2.82	2.38
Ca(17)	6.00	2.32 – 2.58	2.40	Ca(35)	6.00	2.28 – 2.92	2.37
Ca(18)	6.68	2.27 – 2.99	2.48	Ca(36)	6.00	2.29 – 2.54	2.38

The polyhedra about the Ca atoms

The thirty-six Ca atoms in the unit cell may be classified into two groups; eighteen Ca's on the mirror plane and eighteen Ca's located approximately on a plane close to $x, \frac{1}{4}, z$. Although the refinement has revealed that most of Ca's show positional splittings (Table 4), the effect is relatively small for Ca's in the former group, the range of splittings being $0.02(1) \sim 0.52(2)$ Å. In contrast to those, the splittings of Ca's of the latter group tend to be significant, $0.16(1) \sim 0.73(2)$ Å. This situation would probably mean that Ca's in the latter group have more freedom to move compared to those of the former group.

We give in Table 5 the Ca – O bond lengths. For each split Ca atom, the distances are given between the average positions of the split pair and the surrounding oxygen atoms. Since the occupancies of the oxygen atoms are in general smaller than unity because of the orientational disorder of the tetrahedra, each Ca – O bond length was weighted by its occupancy to evaluate the mean Ca – O bond lengths (Table 5). The Ca – O bond lengths are in the range from 2.20 Å to 3.00 Å, giving an over-all mean value of 2.407 Å.

The coordination number of each Ca (as defined by the number of Ca – O $\leq$ 3 Å) was likewise calculated by taking the sum of the bond occupancies. The numbers were found to be $6.0 \sim 7.12$, with a mean of 6.15. This value is to be compared with the average coordination number

6.21 which we calculated for **T** (Golovastikov et al., 1975). There is a little difficulty to evaluate the coordination numbers of Ca's in the structure of **R** (Nishi and Takéuchi, 1984b) because of the complicated mode of the orientational disorder of the tetrahedra. However, one of the three Ca's is essentially fivefold, while other two are sixfold; the mean coordination number may then be regarded as 5.66. The mean coordination number of the present superstructure thus fall in between those of **T** and **R** in conformity with the general trend of inorganic crystal structures in which coordination number tends to decrease with the increase of temperature.

Computations were performed on HITAC M-280H at the Computer Centre of the University of Tokyo.

References

Bigaré, M., Guinier, A., Mazières, C., Regourd, M., Yannaquis, N., Eysel, W., Hahn, Th., Woermann, E.: Polymorphism of tricalcium silicate and its solid solutions. Am Ceram. Soc. **50**, 609–619 (1967)

Busing, W. R., Martin, K. O., Levy, H. A.: ORFLS. Oak Ridge National Laboratory Report ORNL-TM-305 (1962)

Golovastikov, R., Matveeva, R. G., Belov, N. V.: Crystal structure of the tricalcium silicate $3CaO \cdot SiO_2 = C_3S$. Sov. Phys. Crystallogr. **20**, 441–445 (1975)

Jeffery, J. W.: The crystal structure of tricalcium silicate. Acta Crystallogr. **5**, 26–35 (1952)

Maki, I., Chromý, S.: Microscopic study on the polymorphism of Ca_3SiO_5. Cem. Concr. Res. **8**, 407–414 (1978)

Nishi, F., Takéuchi, Y.: Two-layer structure of tricalcium germanate, $Ca_{3-x}[GeO_4](O_{1-2x}, F_{2x})$ with $X \simeq 0.275$. Acta Crystallogr. **C40**, 730–733 (1984a)

Nishi, F., Takéuchi, Y.: The rhombohedral structure of tricalcium silicate at 1200° C. Z. Kristallogr. **168**, 197–212 (1984b)

Nishi, F., Takéuchi, Y.: 24-Layer structure of tricalcium germanate, Ca_3GeO_5. Acta Crystallogr., in the press (1985)

Takéuchi, Y., Nishi, F., Maki, I.: Structural aspects of the phase transitions in tricalcium silicate $Ca_3SiO_5 (= C_3S)$. Acta Crystallogr. **A40**, C215 (1984)